SIMULATION OF AIRFLOW AND PARTICLE DEPOSITION IN THE CENTRAL HUMAN AIRWAYS

D. Fontana*, M. Vanni* and G. Baldi*

* Dipartimento di Scienza dei Materiali e Ingegneria Chimica, Politecnico di Torino, Torino, Italy

marco.vanni@polito.it

Abstract: This work investigates the airflow and deposition of particles in the central part of the bronchial tree (generations 4-15) during the inspiration phase, by means of numerical modelling. The Computational Fluid Dynamics code FLUENT 6.1 with the Eulerian-Lagrangian approach was used to simulate particle trajectories. Particles with diameter of 1, 2, 5, 10, 20 and 50 μm were introduced in a symmetric model of single bifurcation, created on the basis of the morphometric studies by Weibel and by Hammersley and Olson, in order to represent the whole central part of the respiratory system with the same geometry, appropriately scaled down. The particle behaviour was studied in two different conditions of introduction of the discrete phase, and a comparison between particle deposition obtained with and without considering the Saffman lift force was carried out.

Introduction

The therapy of respiratory diseases mostly uses pharmaceuticals in form of aerosol delivered into the lungs: the efficiency and efficacy of the therapy highly depend on the size of the drug particles and their transport and deposition in the respiratory system. Therefore a detailed knowledge of the transport of air and particles in the human lungs is needed to predict accurately the deposition mechanism of aerosol particles in the respiratory airways and consequently the doses needed for the therapy. This is also required for the study of the maximum allowable concentration for particulate in air. Particle deposition in the lungs is not uniform, and particles tend to concentrate in limited zones of the respiratory system. Hence even low concentrations of contaminants may have serious implications in human health.

The airway network has quite small dimension and the smaller airways deep down into the lungs are inaccessible. Numerical modelling offers a tool to reproduce the complexity of the structure and analyse the various aspects that influence the final particle distribution with excellent flexibility.

Lee *et al.* [1] pointed out the necessity of considering at least a double bifurcation to obtain realistic results for air flow and particle deposition, because of the boundary conditions used for the air inlet: generally, the air is introduced with a parabolic profile, but this is not a realistic assumption, since the ducts are not long enough to allow the flow to fully develop; this implies that secondary flows, which play an important role in particle deposition, are neglected when a single bifurcation is considered. According to this consideration, reliable predictions cannot be obtained for the first simulated bifurcation, but only for the subsequent ones. Therefore, after the work of Lee *et al.*, most studies were performed on geometries constituted of at least two successive bifurcations, often considering the two limits of coplanar and orthogonal bifurcations [2,3,4,5]. These works concentrated basically on a limited zone of the respiratory system, often considering only a double bifurcation as computational domain.

The aim of our work is to investigate the airflow and particle deposition in the central part of the bronchial tree (generations 4-15) during the inspiration phase. Particles of different size were introduced in a symmetric model of single bifurcation, generated on the basis of the morphometric studies by Weibel [6] and Hammersley and Olson [7] in order to reproduce the cited zone of the respiratory system with the same geometry, appropriately scaled down. The symmetry in geometry was chosen because, even if less anatomically accurate, it should afford a better understanding of transport phenomena, due to its standardized geometry, since, as highlighted by Hammersley and Olson, a deep knowledge of the fluid mechanic effects induced by each component of airway design is incomplete at this time.

Geometry and Methods

Weibel [6] and Hammersley and Olson [7] showed that bifurcation angles of 70°, a diameter-to-length ratio of 0.30 and a branching diameter ratio between two successive generations equal to 0.80 are typical of all generations between the fourth and the fifteenth one; therefore with these values, by simply scaling the size, any zone of the respiratory system in the cited generation range can be reproduced accurately. The dimensions to model generations 4-5 (the first ones considered in this work) are then: D_4 = 4 mm [6], L_4 = 13 mm, D_5 = 3.2 mm, L_5 = 11 mm. According to the description of Hammersley and Olson, the geometry was realized reproducing 80% of the parent branch as a cylinder and the last 20% as a curved transitional zone; the transitional zone was generated by the Boolean union of a frustum, two tori and the first part of the two

ISSN: 1727-1983

cylinders representing the daughter branches; in order to create this zone with length of $0.2 \cdot L_{parent}$, the curvature radius of the tori was chosen equal to the diameter of the daughter branch; flow divider sharpness was set to $0.1 \cdot D_{daughter}$.

One of the purposes of this work was to analyse the airflow development in the airways, which was not methodically studied by previous researches. Therefore, the simulations were performed in succession, from generation 4 to generation 15, introducing the outlet flow profile of a simulation as inlet for the subsequent one. Before being introduced as boundary condition, the velocity profile was rotated of 90°, in order to represent the mutual orthogonality between two successive bifurcation planes. In fact, inspections of human lung casts and bronchographic images revealed that an azimuthal angle of 90° can create a realistic three-dimensional lung model [8]. Due to the adopted condition, the integration grid was created considering only half length for the ducts. Thus, the domain dimensions for generations 4-5 became: D_4 = 4 mm, L_4 = 6.5 mm, D_5 = 3.2 mm, L_5 = 5.5 mm.

The computational grid, realized with the pre-processor GAMBIT of Fluent Inc., is shown in Figure 1, which also reports the names used subsequently in this paper to indicate the branches. The grid consists of about 80,000 tetrahedral cells. The outlet condition taken as inlet in the subsequent bifurcation was that of the daughter branch *b*; therefore, in order to have more detailed information, the mesh was thickened in this zone (Fig. 1 b and c).

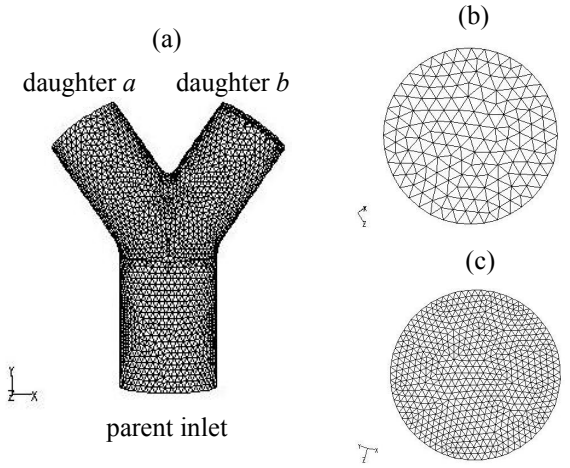

Figure 1: (a) Integration grid; (b) Grid of the daughter airway a; (c) Grid of the daughter airway b

Simulations were performed by means of the Computational Fluid Dynamics code FLUENT v. 6.1.22, based on the finite volume discretisation method. Particle trajectories were calculated by the Eulerian-Lagrangian method, which first solves air flow equations and then calculates the trajectories of the transported particles.

The flow was considered laminar, incompressible and in steady-state conditions (inspiration). The tubes were assumed inelastic and smooth. Transfer of momentum between gas and particles due to drag was neglected, because of the very low volume fraction of the dispersed phase.

In the first simulation (generation 4) a uniform inlet velocity of 2.5 m/s was prescribed, corresponding to a light exercise breathing condition (Q = 30 l/min at trachea), assuming an equal flow division in all branches before generation 4: $Q_4 = \frac{Q}{2^4} = 1.875$ l/min, $|\mathbf{v}_4| = \frac{Q_4}{\pi D_4^2 / 4} = 2.5$ m/s. An equal flow division in the branches was assumed also for the subsequent generations, specifying two outflow boundary conditions at the flow exits, each with a fractional flow rate equal to 0.5. Nowak *et al.* [9] showed that the outflow approximation yields an insignificant deviation from particle tracking calculations made with constant pressure outlet boundary conditions (which are more physiologically realistic, since the air flow is driven by the pressure at the end of the lung airways); moreover, the outflow condition can be also used to simulate the cases of downstream airway obstruction.

Spherical particles of density 1 g/cm^3 with diameters of 1, 2, 5, 10, 20 and 50 μm were introduced in the domain from the inlet of the parent branch. A comparison between particle deposition obtained with and without considering the Saffman lift force was carried out. Two different methods of introducing the discrete phase were compared: the first one consisted of introducing the particles with uniform distribution on the whole inlet surface and with a uniform velocity equal to the mean velocity of the inlet air; in the second one the spatial distribution and velocity of the particles were set equal to those at the exit of the preceding simulation, after being rotated of 90°, in order to reproduce the mutual orthogonality of two subsequent bifurcations. In both cases particle trapping when reaching the wall was assumed.

At a first sight the latter model (non-uniform inlet distribution) appears closer to the physical situation; yet it should be considered that it assumes a sort of perfectly "frozen" configuration of the respiratory airways, which may not correspond exactly to the actual situation. Deformation and relative displacement of the different parts of the airways can induce some drift of the particles with respect to the predictions of the non-uniform inlet model. This is why we considered also the condition of uniform inlet distribution of particles, which corresponds to a complete mixing of the particles between different subsequent generations. Of course the two situations are extreme cases and the actual condition is likely to lie in between.

In the uniform inlet distribution the prescribed particle inlet velocity may be different from the actual one; in order for the simulation to be reliable, this effect must be confined to a small portion of the system, close to the entrance, and the particles must reach their proper velocity quite soon. This occurs when the particle response time $\tau_p = \frac{\rho_p d_p^2}{18\mu}$ is much smaller than the

ISSN: 1727-1983

particle residence time $\tau_i \approx V_i / Q_i$ (where V_i indicates the volume and Q_i the flow rate of the *i*-th generation, respectively). As highlighted in Tables 1 and 2, this is true for particles with $d_p \leq 10$ μm, for which $\tau \geq 10\tau_p$, and also for particles with $d_p = 20$ μm, for which $\tau > 5\tau_p$. For bigger particles the condition is not satisfied and thus the uniform inlet approach is not reliable.

Table 1: Particle response time vs size

d_p [μm]	τ_p [s]
1	$3{,}10 \cdot 10^{-6}$
2	$1{,}24 \cdot 10^{-5}$
5	$7{,}76 \cdot 10^{-5}$
10	$3{,}10 \cdot 10^{-4}$
20	$1{,}24 \cdot 10^{-3}$
50	$7{,}76 \cdot 10^{-3}$

Table 2: Particle residence time at each generation

Generation number	τ_i [s]
4	$5{,}06 \cdot 10^{-3}$
5	$5{,}18 \cdot 10^{-3}$
6	$5{,}31 \cdot 10^{-3}$
7	$5{,}44 \cdot 10^{-3}$
8	$5{,}57 \cdot 10^{-3}$
9	$5{,}70 \cdot 10^{-3}$
10	$5{,}84 \cdot 10^{-3}$
11	$5{,}98 \cdot 10^{-3}$
12	$6{,}12 \cdot 10^{-3}$
13	$6{,}27 \cdot 10^{-3}$
14	$6{,}42 \cdot 10^{-3}$
15	$6{,}57 \cdot 10^{-3}$

Results and discussion

Velocity field

Before starting the analysis of the airflow development in the airways, the computational method was validated comparing axial velocity profiles at the end of the fifth generation branch with those obtained experimentally by Zhao and Lieber [10], who studied the steady inspiratory flow in a single bifurcation system representing a major bronchial bifurcation. Comparison were made with the profiles at station 17 (where the tube has become cylindrical) and Re = 518 (the nearest to the condition at generation 5: Re = 426) of the work of Zhao and Lieber. As highlighted in Figure 2, the agreement is good both in the bifurcation plane and in the plane orthogonal to the bifurcation.

Figure 3 shows the dimensionless axial velocity profiles in the middle of the fifth, eighth, tenth, twelfth and fifteenth generations. It is well discernible that the maximum of the profile in the bifurcation plane shifts towards the centre of the bifurcation and the "M" shape in the plane orthogonal to the bifurcation, typical of the first generations of the respiratory system [3,4,10,11], turns into a parabolic profile. This behaviour was expected: Liu *et al.* [4], who investigated flow patterns and pressure drop in generations 5-7 (Weibel's A model [6]) as a function of the Reynolds number, showed that when Re becomes < 200, the "M" shape disappears and the shifted maximum tends to move towards the axis of the branch. Table 3 reports the Reynolds numbers for each generation (Re are based on the inlet diameter and the mean inlet velocity). At generation 8 (Re = 104) the "M" shape is practically disappeared and the profile becomes completely parabolic from generation 10 (Re = 41), after which it does not change anymore; in the bifurcation plane, as also observed by Liu *et al.*, the profile transformation is slower, anyway it leads to a symmetric parabolic profile at generation 12.

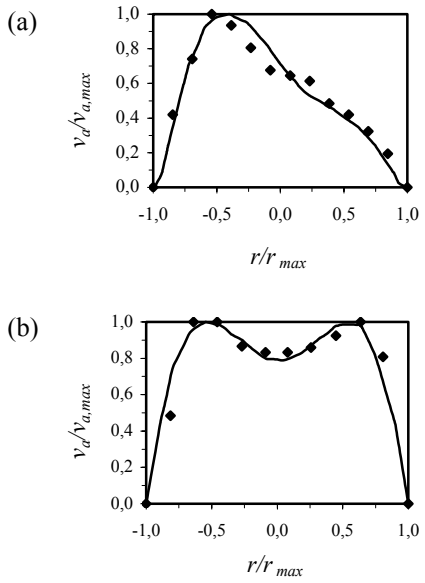

Figure 2: Comparison of velocity profiles with Zhao and Lieber [9]. (———) simulations; (♦) Zhao and Lieber. (a) Bifurcation plane; (b) Plane orthogonal to the bifurcation

Table 3: Reynolds numbers at the analysed generations

Generation number	Re
4	685
5	426
6	266
7	166
8	104
9	65
10	41
11	25
12	16
13	10
14	6
15	4

The reason of such a behaviour can be explained by analysing the development of secondary flows along the respiratory airways (Fig. 4). Zhao and Lieber [10] and Comer *et al.* [3] concluded that the skewed profile in the bifurcation plane is caused by vortices, that move the fluid from the outer wall of the bifurcation to the flow divider; the presence of two symmetric vortices induces the presence of the "M" shape in the transverse plane. This couple of vortices is clearly discernible at generation 5 (Fig. 4a), but progressively disappears in

ISSN: 1727-1983

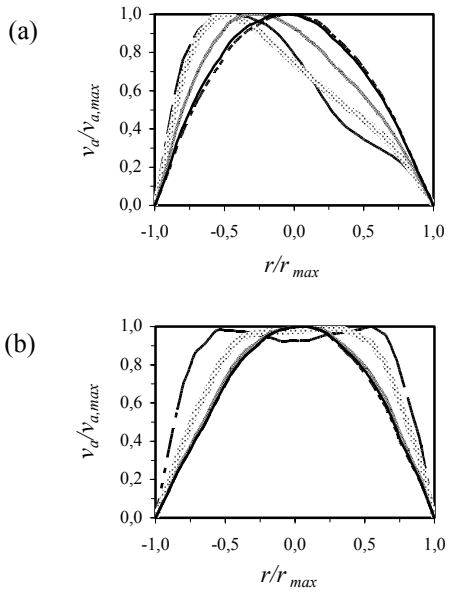

Figure 3: Dimensionless inlet flow profiles at generation 5 (– - - – - -), generation 8 (·····), generation 10 (~~~~~), generation 12 (———) and generation 15 (- - - - - - - -). (a) Bifurcation plane; (b) Plane orthogonal to the bifurcation

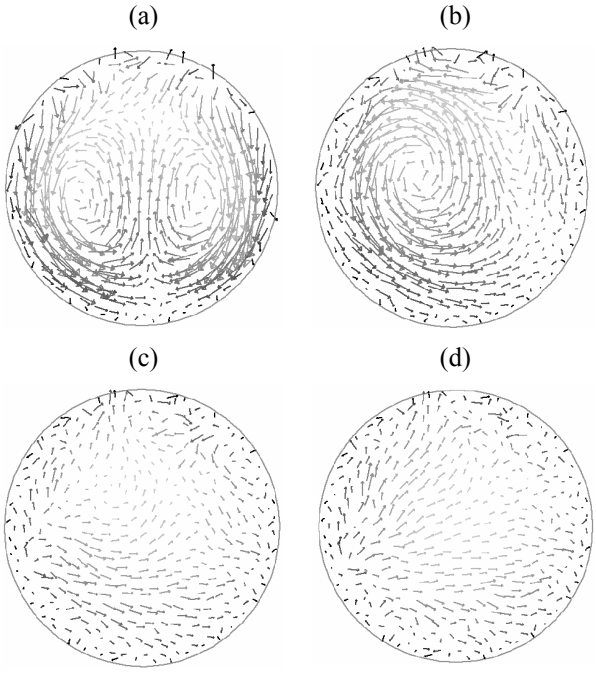

Figure 4: Secondary velocities at the inlet of the domain. (a) Generation 5; (b) Generation 8; (c) Generation 10; (d) Generation 12

the subsequent generations. At generation 8 (Fig. 4b) a main vortex which moves the fluid towards the centre of the bifurcation is still present and therefore the velocity maximum in the bifurcation plane is still shifted towards the flow divider; however, the secondary flow has lost its symmetry, causing the formation of a nearly flat profile at the centre of the tube in the transverse plane (instead of the "M" shaped profile). From generation 10 (Fig. 4c), the vortex disappears and the secondary motions change their direction, moving the fluid towards the axis of the branch and therefore shifting the velocity maximum in that direction; the low-speed flow tends to move towards the outside of the duct, causing the progressive transformation of the "M" shape to a parabola.

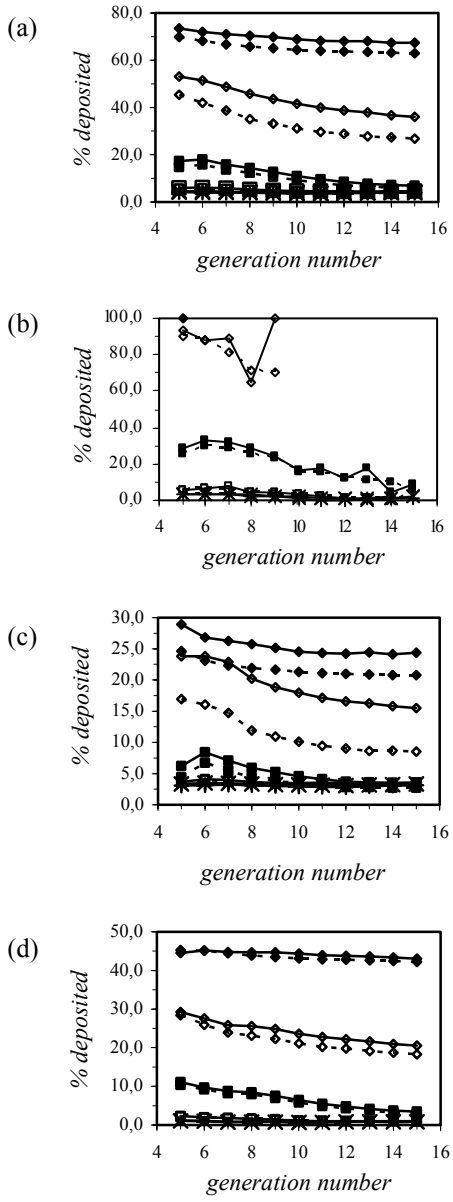

Figure 5: Deposited particles/particles tracked at each generation. (a) Branch + carina, uniform distribution; (b) Branch + carina, non uniform distribution; (c) Branch, uniform distribution; (d) Carina, uniform distribution . (——): lift force; (- - - -): no lift force. +: 1 μm; ×: 2 μm; □: 5 μm; ■: 10 μm; ◊: 20 μm; ♦: 50 μm

Particle deposition

As highlighted in Figure 5, reporting the ratio between deposited particles and tracked particles at each generation, the presence of the Saffman lift force

ISSN: 1727-1983

influences only the behaviour of the biggest particles in the case of uniform inlet distribution (Figure 5a), and does not influences at all the particle behaviour in the case of non uniform inlet distribution (Figure 5b). In the former case the effect, for particles with diameter $d_p \geq$ 10 μm, is an increase of the deposition when the lift force is considered; this increase can reach 30% (d_p = 20 μm). As expected, the effect is higher for the deposition in the branches than on the bifurcation ridge (carina) (Figure 5c,d): the increase in particle deposition in branches can even arrive at 100%. However, this difference is practically not detectable if we refer the number of particles deposited at each generation to the number of particles entering generation 4 (Figure 6). Moreover, particles of every size deposit mainly on the carina, where the effect of the lift force is negligible (Figure 5d). Therefore, since the aim of works like ours is to determine the locations of higher particle deposition and the particle concentration in such zones, we can conclude that simulations can be made neglecting the effect of the lift force.

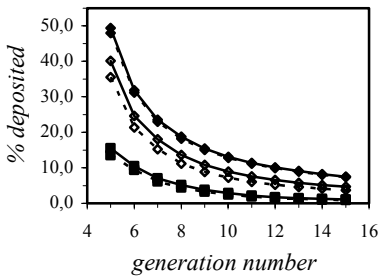

Figure 6: Deposited particles/particles entering generation 4, uniform distribution. (——): lift force; (- - - -): no lift force. ■: 10 μm; ◊: 20 μm; ♦: 50 μm

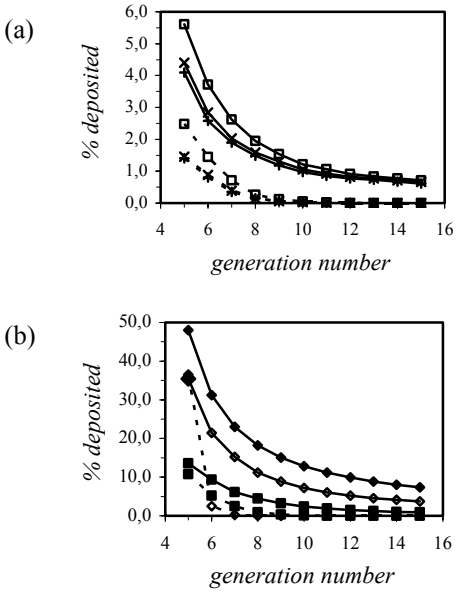

Figure 7: Deposited particles/particles entering generation 4, no lift force. (——): uniform distribution; (- - - -): non uniform distribution. (a) +: 1 μm; ×: 2 μm; □: 5 μm; (b) ■: 10 μm; ◊: 20 μm; ♦: 50 μm

It is instead interesting to note the huge difference in particle deposition between the two methods of introduction of the discrete phase (Figure 7): the deposition calculated by the uniform inlet distribution is always higher than that calculated by the non uniform one. It was observed that the non uniform inlet distribution implies that, after the eighth generation, most particles concentrate in the middle of the branch section, where the air velocity is higher, and therefore the probability of impacting the wall is smaller. This would explain the smaller deposition rate for the non uniform distribution.

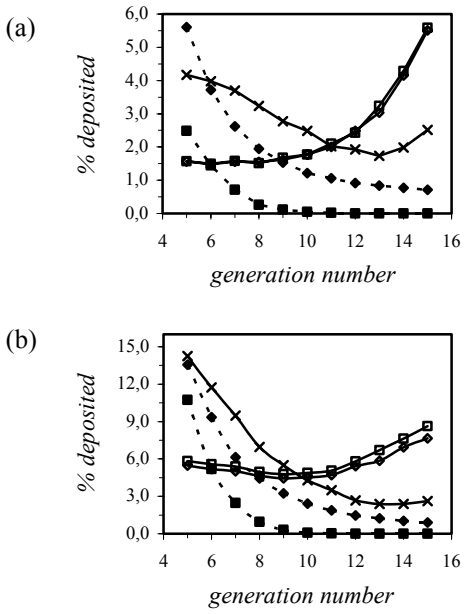

Figure 8: Deposited particles/particles entering generation 4. (a) d_p = 5 μm; (b) d_p = 10 μm. (—◊—): Martonen V_T = 500 ml, f = 30 min^{-1}; (—□—): Martonen V_T = 1000 ml, f = 15 min^{-1}; (—×—): Martonen V_T = 1500 ml, f = 30 min^{-1}; (- - ♦ - -): uniform inlet; (- - ■ - -): non uniform inlet

Thus, it was necessary to compare our results with those found in the literature, in order to understand which approach is more accurate. Figure 8 reports the comparison between our results for 5 and 10 μm particles and the predictions of the models by Martonen *et al.* [12], who calculated the particle deposition for the whole respiratory system at three respiratory conditions (tidal volume V_T = 500 ml and breathing frequency f = 30 min^{-1} ⇒ Q = 15 l/min; V_T = 1000 ml and f = 15 min^{-1} ⇒ Q = 15 l/min; V_T = 1500 ml and f = 30 min^{-1} ⇒ Q = 45 l/min). Their work was validated by comparison with the experimental data of Heyder *et al.* [13]. We decided to compare our predictions with those of Martonen *et al.* instead of those of Heyder *et al.* because the data of Martonen *et al.* are also reported on a generation-by-generation basis, whereas those of Heyder *et al.* only as deposition in larger regions (total deposition, tracheobronchial deposition, pulmonary deposition), and therefore it was difficult to find a correspondence between our generations and the regions of Heyder *et*

ISSN: 1727-1983

al.; anyway, the fit between the data of Martonen *et al.* and those of Heyder *et al.* is very good, hence comparison of our results with those of Martonen *et al.* is not significantly different from comparison with those of Heyder *et al.* It appears from Figure 8 that the particle deposition is predicted better by the uniform inlet distribution than by the non uniform one. There are some differences between our predictions with the uniform distribution and those of Martonen *et al.*, which may be due either to the differences in the air flow rate or to the fact that we did not consider the deposition in the earlier generations: maybe the particle history partly affects the results. Anyway, this comparison allows one to conclude that the uniform distribution is more accurate than the non-uniform one for particles with diameter until around 10 μm. Moreover, a qualitative comparison with the reference values for regional deposition provided by ICRP [14] shows that the uniform inlet distribution is the more reliable also for particles of diameter until 20 μm: it predicts that these particles can reach the respiratory zone (from generation 16 to alveoli), in agreement with the reference values of ICRP, whereas the non uniform distribution calculates complete deposition before generation 10.

Conclusions

Simulations of the airflow showed a relevant change in the velocity profiles during the passage in the airways, because of the transformation of secondary flows along the respiratory airways.

Simulations of the particle deposition pointed out that the effect of the Saffman lift force can be neglected and that the more accurate method of introducing the discrete phase is the uniform distribution, even if at a first sight the non uniform distribution may appear more realistic. The latter result is very interesting if seen on respect of the computational time: the non uniform inlet method needs a much larger number of particles to reproduce the behaviour in the lungs (the number of particles decreases as they pass through the generations, because only the particles at the exit of the daughter branch *b* are introduced in the following simulation); as a consequence, the computational time increases dramatically.

The simulations showed that only a small portion of particles of diameter up to 10 μm deposits in the conductive zone (the total deposition in generations 5-15 is less than 10% for d_p = 1-5 μm and of 17% for d_p = 10 μm); the deposition of particles with diameter of d_p = 20 μm is of about 50% in the analysed generations; particles with diameter of 50 μm do not reach the respiratory zone. The deposition is always higher on the carina, where from 60% to 80% of the total deposited particles stop, except for particles of 1 μm, for which the percentage of deposition is of 20%.

References

[1] LEE J.W., GOO J.H., CHUNG M.K. (1996): 'Characteristic of Inertial Deposition in a Double Bifurcation', *J. Aerosol Sci.*, **27 (1)**, pp. 119-138

[2] LEE J.W., LEE D.Y., KIM W.S. (2000): 'Dispersion of an Aerosol Bolus in a Double Bifurcation', *J. Aerosol Sci.*, **31 (4)**, pp. 491-505

[3] COMER J.K., KLEINSTREUER C., KIM C.S. (2001): 'Flow Structures and Particle Deposition Patterns in Double-Bifurcation Airway Models. Part 1. Air Flow Fields', *J. Fluid Mech.*, **435**, pp. 25-54

[4] LIU Y., SO R.M.C., ZHANG C.H. (2002): 'Modeling the Bifurcation Flow in a Human Lung Airway', *Journal of Biomechanics.*, **35**, pp. 465-473

[5] BALÁSHÁZY I., FARKAS Á., SZÖKE I. (2003): 'Simulation of Airflow, Aerosol Deposition and Clearance in Central Human Airways', Proc. of 5th International Technion Symposium "Technology for Peace – Science for Mankind", Vienna, 2003, Internet site address: http://www.technion.org/Pages/pdf/B_P4.pdf

[6] WEIBEL E.R. (1963): 'Morphometry of the Human Lung', (Academic Press, New York)

[7] HAMMERSLEY J.R., OLSON D.E. (1992): 'Physical Models of the Smaller Pulmonary Airways', *J. Appl. Physiol.*, **72 (6)**, pp. 2402-2414

[8] KITAOKA H., TAKAKI R., SUKI B. A. (1999): 'Three-Dimensional Model of the Human Airway Tree', *J. Applied Physiol*,. **87**, pp. 2207-2217

[9] NOWAK N., KAKADE P.P., ANNAPRAGADA A.V. (2003): 'Computational Fluid Dynamics of Airflow and Aerosol Deposition in Human Lungs', *Ann. Biomed. Eng.*, **31**, pp. 374-390

[10] ZHAO Y., LIEBER B.B. (1994): 'Steady Inspiratory Flow in a Model Symmetric Bifurcation', *Transactions of the ASME*, **116**, pp. 488-496

[11] RAMUZAT A., RIETHMULLER M.L. (2002): 'PIV Investigation on Oscillating Flows within a 3D Lung Multiple Bifurcations Model', Proc. Of 11th International Symposium on Application of Laser Techniques to Fluid Mechanics, Lisbon, 2002

[12] MARTONEN TB, MUSANTE CJ, SEGAL RA, SCHROTER JD, HWANG D, DOLOVICH MA, BURTON R, SPENCER M, FLEMING JS. (2000): 'Lung Models: Strengths and Limitations', Proc. of the Consensus Conference on Aerosol and Delivery Devices, Bermuda, 1999. *Respir. Care.* **45**, pp. 712-736

[13] HEYDER J., GEBHART J., RUDOLF G., SCHILLER C.F., STAHLHOFEN W. (1986): 'Deposition of Particles in the Human Respiratory Tract in the Size Range 0.005-15 μm', *J. Aerosol Sci.* **17**, pp. 811-825

[14] ICRP Supporting Guidance 3 (2002): 'Guide for the Practical Application of the ICRP Human Respiratory Tract Model', *Ann. ICRP.* **32 (1-2)**, pp. 1-312

ISSN: 1727-1983